handling, or safety procedures. The greatest potential may lie in the ability to fluorinate aryl anions. The ability to selectively generate the anions of a broad variety of aromatic compounds has been well established, and other methods for the direct fluorination of aromatics remain limited, especially for electron-deficient systems.

Acknowledgment. Helpful discussions with B. E. Smart, A. E. Feiring, and S. Rozen are appreciated, along with the technical assistance of H. J. Lindy and D. R. Sanderson.

Registry No. 1, 88303-12-2; **2**, 88303-13-3; **3**, 88303-14-4; **4**, 88303-15-5; **5**, 88303-16-6; **6**, 88303-17-7; **7**, 88303-18-8; $PhCF(COOEt)_2$, 2802-98-4; $CH_3CF(COOEt)_2$, 16519-02-1; PhF, 462-06-6; $CH_3(CH_2)_{13}F$, 593-33-9; $(CH_3)_2CF(NO_2)$, 421-55-6; $Ph_2CFCOOCH_3$, 309-44-4; $PhCH(COOEt)_2$, 83-13-6; $CH_3CH(COOEt)_2$, 609-08-5; PhMgBr, 100-58-3; $CH_3(CH_2)_{13}MgBr$, 88303-25-7; $(CH_3)_2CH(NO_2)$, 79-46-9; $Ph_2CHCOOH$, 117-34-0; 2-fluoro-1-naphthol, 56874-95-4; *N*-(*tert*-butyl)-2-fluoro-4-methylbenzenesulfonamide, 88303-19-9; 3-fluoroanisole, 456-49-5; 2-fluoro-3,3,5,5-tetramethylcyclohexanone, 37783-39-4; 2-fluoroisobutyrophenone, 71057-10-8; 1-fluoroindene, 88303-20-2; 7-chloro-3-fluoro-1-methyl-5-phenyl-1*H*-1,4-benzodiazepin-2-one N^4-oxide, 60628-73-1; *N*-methyl-*p*-toluenesulfonamide, 640-61-9; *N*-(*exo*-2-norbornyl)-*p*-toluenesulfonamide, 88303-21-3; *N*-(*endo*-2-norbornyl)-*p*-toluenesulfonamide, 88303-22-4; *N*-(*tert*-butyl)-*p*-toluenesulfonamide, 2849-81-2; *N*-cyclohexyl-*p*-toluenesulfonamide, 80-30-8; *N*-neopentyl-*p*-toluenesulfonamide, 88303-23-5; *N*-neopentylbutanesulfonamide, 88303-24-6; 1-naphthol, 90-15-3; anisole, 100-66-3; 3,3,5,5-tetramethyl-1-cyclohexen-1-ol acetate, 56763-68-9; isobutyrophenone, 611-70-1; indene, 95-13-6; 7-chloro-1-methyl-5-phenyl-1*H*-1,4-benzodiazepin-2-one N^4-oxide, 2888-64-4.

Photolysis of 3-Chlorodiazirine in the Presence of Alkenes. Kinetic Evidence for Intervention of a Carbene–Alkene Intermediate in Addition of Chlorocarbene to Alkene

Hideo Tomioka,* Norihiro Hayashi, and Yasuji Izawa

Department of Industrial Chemistry
Faculty of Engineering, Mie University
Tsu, Mie 514, Japan

Michael T. H. Liu

Department of Chemistry
University of Prince Edward Island
Charlottetown, Prince Edward Island, Canada C1A 4P3

Received May 20, 1983

During the course of the studies on the competition between intramolecular 1,2-H shift and intermolecular addition of benzylchlorocarbene to alkene, we obtained chemical evidence for the intervention of a reversibly formed dissociable intermediate in the addition of carbene to alkene, as has been suggested[1] by Turro and Moss in their spectrophotometric studies.

Irradiation of 3-benzyl-3-chlorodiazirines (**1**) in cyclohexane was carried out with a 300-W high-pressure Hg lamp at 10 °C until all of the diazirine was destroyed. A Corning CS-052 filter cutoff at 350 nm was used in order to avoid product isomerization. The photolysis products of **1** were exclusive (*Z*)- and (*E*)-β-chlorostyrenes apparently arising from a 1,2-H shift in the photolytically generated chlorocarbene **2**. When the irradiation of **1** was carried out in the presence of alkenes **4**, 1,2-H migration was appreciably suppressed concomitant with the formation of cyclopropanes **5** (see Table I and Scheme I). Addition of the carbene to (*Z*)-4-methyl-2-pentene was stereospecific within the limit of GC detection. This is consistent with the earlier observation[2] that the singlet chlorocarbene is involved in the cyclopropanation.

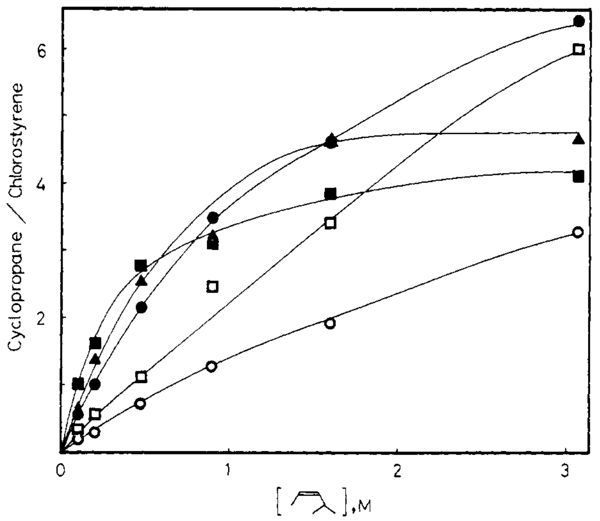

Figure 1. The ratio of intermolecular to intramolecular products as a function of alkene concentration in the reaction of $ArCH_2\ddot{C}Cl$ with (*Z*)-4-methyl-2-pentene: (●) C_6H_5-, (□) $4\text{-}MeC_6H_4-$, (▲) $4\text{-}ClC_6H_4-$, (■) $3,4\text{-}Cl_2C_6H_3-$, (○) $4\text{-}MeOC_6H_4-$.

Scheme I

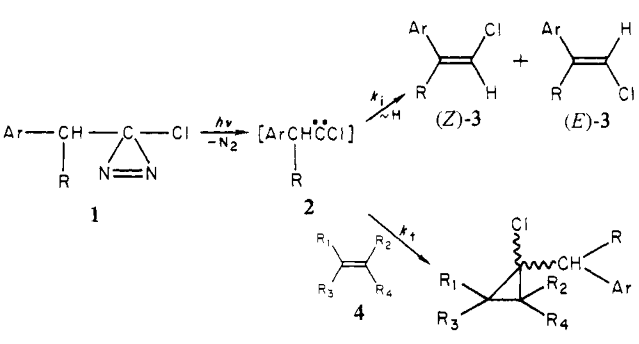

The intermolecular/intramolecular product ratio (**5**/**3**) varies sensibly with both carbenic and olefinic substitutents, but inspection of the product distributions observed in neat alkene (Table I) did not lead to a relevant structure–reactivity relationship. For example, the product ratio **5**/**3** in the reaction of substituted benzylchlorocarbene **2b–f** with (*Z*)-4-methyl-2-pentene decreased in the order H > 4-Me > 4-Cl > 4-MeO > $3,4\text{-}Cl_2$, while the order expected from hydride character[2e,3,4] of the 1,2-H migration was $3,4\text{-}Cl_2$ > 4-Cl > H > 4-Me > 4-MeO. Examination of the product distribution as a function of alkene concentration showed, however, that the order of the product ratio **5**/**3** changed with the alkene concentration. Thus, a plot of the intermolecular/intramolecular product ratio (**5**/**3**) as a function of alkene concentration (e.g., Figure 1) shows pronounced curvature. This cannot be explained in terms of a usual kinetic model for the competitive intermolecular–intramolecular processes for carbene **2** as in Scheme I, which predicts the product ratio **5**/**3** is a linear function of alkene (A) concentration. The results can be better interpreted in terms of a kinetic model recently suggested[1] by

---

(1) (a) Turro, N. J.; Butcher, J. A., Jr.; Moss, R. A.; Guo, W.; Munjal, R. C.; Fedorynski, M. *J. Am. Chem. Soc.* **1980**, *102*, 7576. (b) Turro, N. J.; Lehr, G. F.; Butcher, J. A., Jr., Moss, R. A.; Guo, W. *Ibid.* **1982**, *104*, 1754. (c) Moss, R. A.; Perez, L. A.; Turro, N. J.; Gould, I. R.; Hacker, N. P. *Tetrahedron Lett.* **1983**, *24*, 685.

(2) (a) Moss, R. A.; Fantina, M. E. *J. Am. Chem. Soc.* **1978**, *100*, 6788. (b) Moss, R. A.; Fantina, M. E.; Munjal, R. C. *Tetrahedron Lett.* **1979**, 1277. (c) Moss, R. A.; Munjal, R. C. *Ibid.* **1980**, *21*, 2037. (d) Moss, R. A.; Wetter, W. P. *Ibid.* **1981**, *22*, 997. (e) Moss, R. A.; Munjal, R. C. *J. Chem. Soc., Chem. Commun.* **1978**, 755.

(3) Su, D. T. T.; Thornton, E. R. *J. Am. Chem. Soc.* **1978**, *100*, 1872.

(4) Tomioka, H.; Okuno, H.; Kondo, S.; Izawa, Y. *J. Am. Chem. Soc.* **1980**, *102*, 7123.

0002-7863/84/1506-0454$01.50/0 © 1984 American Chemical Society

Table I. Product Distribution from the Reaction of Chlorocarbene (2) with Alkenes[a]

2	alkene 4	yield, %[b] 3 (*E*/*Z*)	5 (isomer ratio)[c]	5/3
$C_6H_5CH(Me)\ddot{C}Cl$ (a)	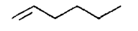	67.4 (3.24)	14.1 (0.21)	0.21
		63.8 (2.91)	29.7 (1.18)	0.47
	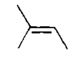	64.9 (2.55)	33.3 (8.51)	0.50
$C_6H_5CH_2\ddot{C}Cl$ (d)	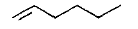	14.6 (2.40)	70.8 (4.75)	4.85
		12.4 (1.88)	85.3 (14.2)	6.88
	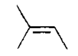	13.5 (1.50)	86.6 (3.42)	6.41
$4\text{-}MeOC_6H_4CH_2\ddot{C}Cl$ (b)		16.3 (6.81)	80.9 (24.3)	4.93
$4\text{-}MeC_6H_4CH_2\ddot{C}Cl$ (c)		2.8 (3.92)	84.7 (17.8)	6.62
$4\text{-}ClC_6H_4CH_2\ddot{C}Cl$ (e)		15.4 (2.28)	84.5 (20.1)	5.49
$3,4\text{-}Cl_2C_6H_3CH_2\ddot{C}Cl$ (f)		22.9 (4.20)	77.1 (21.0)	3.37

[a] Irradiations were performed on a 10 mM solution of diazirine 1 in neat alkene 4 at 10 °C through a Corning CS-052 filter. Product cyclopropanes were identified by structurally consistent IR and NMR spectra and by mass spectroscopic analyses. [b] Determined by GC. Average of dublicate runs are tabulated; reproducibility was <±5%. [c] Ratio of two GC peaks corresponding to cyclopropane 5; the major isomer eluted first in a 4.0 mm × 2.0 m column packed with 5% PEG 20 M on 60-80 mesh Uniport B.

Table II. Relative Rate Constants for the Reaction of Chlorocarbene 2 with Alkene

2	alkene 4	k_i/k_2	k_i/k_t(rel)
$C_6H_5CH(Me)\ddot{C}Cl$ (a)		3.00 ± 0.78	6.57 ± 0.72 (39.3)
$4\text{-}MeOC_6H_4CH_2\ddot{C}Cl$ (b)	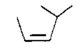	0.204 ± 0.0054	0.557 ± 0.0037 (3.3)
$4\text{-}MeC_6H_4CH_2\ddot{C}Cl$ (c)		0.139 ± 0.0035	0.298 ± 0.0024 (1.8)
$C_6H_5CH_2\ddot{C}Cl$ (d)		0.118 ± 0.0022	0.0768 ± 0.00026 (0.45)
		0.112 ± 0.0034	0.167 ± 0.0043 (1.0)
	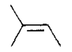	0.136 ± 0.0030	0.747 ± 0.00035 (4.5)
$4\text{-}ClC_6H_4CH_2\ddot{C}Cl$ (e)		0.140 ± 0.0055	0.132 ± 0.00054 (0.80)
$3,4\text{-}Cl_2C_6H_3CH_2\ddot{C}Cl$ (f)	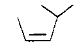	0.235 ± 0.0021	0.073 ± 0.0019 (0.44)

Turro and Moss for the reaction of phenylchlorocarbene and an alkene, which is represented by Scheme II, where $[ArCH_2\ddot{C}Cl\cdots A]$

Scheme II

$$\underset{3}{\mathrm{ArCH{=}CHCl}} \xleftarrow{k_i} \underset{2}{\mathrm{ArCH_2\ddot{C}Cl}} + \mathrm{A} \underset{k_{-1}}{\overset{k_1}{\rightleftharpoons}}$$

$$\underset{6}{[\mathrm{ArCH_2CCl\cdots A}]} \xrightarrow{k_2} \underset{5}{\text{cyclopropane}}$$

is a reversibly formed dissociable intermediate. It follows from Scheme II that

$$\frac{3}{5} = \frac{k_i}{k_2} + \frac{k_i}{k_1k_2[1/(k_{-1}+k_2)][A]} = \frac{k_i}{k_2} + \frac{k_i}{k_t}\frac{1}{[A]} \qquad (1)$$

where $k_1k_2/(k_{-1}+k_2)$ equals the overall rate constant for the trapping process (k_t). The dependence of the product ratio on the concentrations of alkene completely agrees with eq 1. Thus, the plots of 3/5 vs. the reciprocal of alkene concentration give a fairly linear correlation coefficients $r > 0.98$ (e.g., Figure 2). From the slopes and intercepts of such plots, values of k_i/k_2 and k_i/k_t are readily extracted by least-squares linear-regression analysis and are reported in Table II.

In contrast to rather confusing data obtained in neat alkene (Table I), the k_i/k_t values of Table II show that the chlorocarbene 2 is responsive to the substitution patterns of substrates as well as carbene itself. Thus k_i/k_t of the chlorocarbenes 2 decreased as the number of alkyl substituents on the olefinic π-bond increased. This is consistent with the idea that carbenes are generally

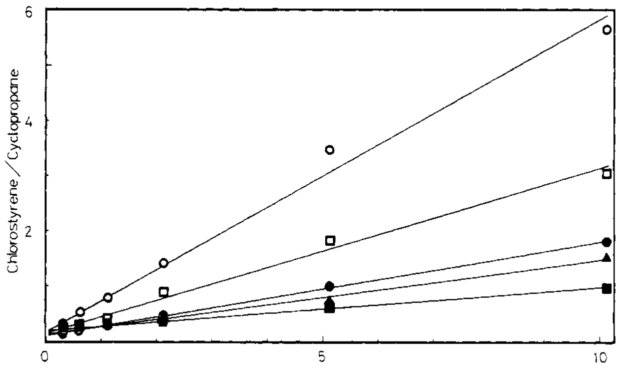

Figure 2. Plot of the ratio of intramolecular to intermolecular products vs. the reciprocal of alkene concentration.

electrophiles in their addition reactions with alkenes. A sharp decrease in k_i/k_t was observed when R in **1** was changed from Me to H. Similar trends are also observed when aryl substituents (X) in **1** (R = H) are successively changes from electron-withdrawing (Cl) to electron-donating (MeO) groups (see Table II). This supports the idea[2e,3,4] that there is substantial hydride character associated with the migrating hydrogen and concomitant positive charge development at the origin of the migration.[5]

---

(5) The substituent effects on the intercepts k_i/k_2 are rather unexpected. Assuming that k_2 is not affected by substituents on the α-phenyl ring, one would expect that the values of k_i/k_2 should be decreased as the ring substituents are changed from electron-donating to -withdrawing groups. Observed parabolic deviations from linearity may imply that intermolecular process is not unaffected by the ring substituent. Presumably, orientation of the phenyl group may affect the electronic as well as steric nature of the chlorocarbene.

Chemistry of New Heteronuclear Bridging Hydrides: $(\mu\text{-H})[Fe(CO)_4M(CO)_5]^-$ (M = Cr, Mo, W)

Larry Arndt, Terry Delord, and Marcetta Y. Darensbourg*

Department of Chemistry, Texas A&M University
College Station, Texas 77843

Received September 16, 1983

The prevalence of hydride ligands at centers of metal aggregation is a well-known feature of transition-metal hydride chemistry.[1] In fact the chemistry of the VIB carbonyl hydrides is dominated by bridging hydrides, $(\mu\text{-H})M_2(CO)_{10}^-$ (M = Cr, Mo, W), in which the hydride bridge is supported neither by a M–M bond nor by bridging carbonyls.[2] In contrast, the structure of $(\mu\text{-H})Fe_2(CO)_8^-$ contains two bridging CO groups as well as an Fe–Fe bond.[3] Although the chemistry of heteronuclear bridging hydrides should prove important to the establishment of relative M–H bond stabilities and metal-to-metal hydride-transfer capabilities, only a few have been well characterized.[4,5] Our studies of the highly reactive monomeric VIB carbonyl hydrides, $HM(CO)_5^-$,[6] indicate that they are good sources of H^- with the ability to transfer H^- to both carbon and metal centers. Pursuant of such chemical characterizations we detected in the reaction of $HW(CO)_5^-$ with $Fe(CO)_5$ the iron formyl, $HC(O)Fe(CO)_4^-$, the iron hydride, $HFe(CO)_4^-$, $(\mu\text{-H})W_2(CO)_{10}^-$, and, as well, a new species believed to be the heteronuclear bimetallic $(\mu\text{-H})FeW(CO)_9^-$, **1c**$^-$. In subsequent work a clean synthesis of the title anions was developed, a preliminary X-ray structural analysis of PPN$^+$**1c**$^-$ has been done,[7] and some interesting and unanticipated chemical reactivity patterns have been observed.

An efficient synthesis (80–90% yield) of $PPN^+(\mu\text{-H})FeM(CO)_9^-$ (M = Cr, Mo, W) is based on the aggregation of $HFe(CO)_4^-$ with photochemically generated $THF{\cdot}M(CO)_5$ (eq 1).

$$THF{\cdot}M(CO)_5 + PPN^+HFe(CO)_4^- \xrightarrow[\text{room temperature}]{\text{THF}} PPN^+(\mu\text{-H})FeM(CO)_9^- \quad (1)$$

1a$^-$, M = Cr; **1b**$^-$, M = Mo; **1c**$^-$, M = W

Following methanol precipitation of excess $PPN^+HFe(CO)_4^-$, filtration, and partial solvent removal, addition of hexane precipitated the product as a yellow or yellow-orange powder. Recrystallization from concentrated methanol/hexane solutions yielded analytically pure samples.[8] As solids these salts may be handled in air for short periods; solutions are air sensitive.

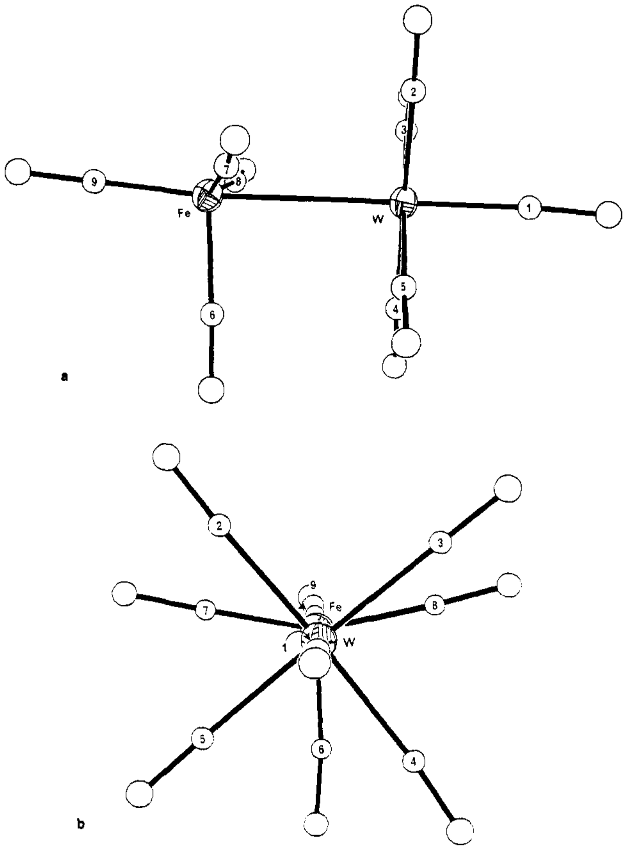

Figure 1. (a) ORTEP drawing of $(\mu\text{-H})FeW(CO)_9^-$ showing 50% probability ellipsoids of the W and Fe atoms. Carbons and oxygens are drawn as spheres. The W is in an octahedral setting with all C–W–C bond angles in the range 87.8–91.4°. Pertinent bond lengths and bond angles: Fe–W, 2.989 (2); W–C1, 1.92 (2); W–C2, 2.05 (2); W–C3, 2.01 (2); W–C4, 2.03 (2); W–C5, 2.05 (2); Fe–C6, 1.81 (2); Fe–C7, 1.81 (2); Fe–C8, 1.74 (2); Fe–C9, 1.75 (2) Å; C7–Fe–C6, 99.2 (7)°; C8–Fe–C6, 101.6 (7)°; C8–Fe–C7, 147.6 (8)°; C9–Fe–C6, 99.5 (7)°; C9–Fe–C7, 100.2 (8)°; C9–Fe–C8, 100.4 (7)°. (b) An end-on view of $(\mu\text{-H})FeW(CO)_9^-$ showing the linear, staggered nature of the heterobimetallic.

The complex ν(CO) IR spectra of all **1**$^-$ show no bands in the bridging CO region.[8] The ^{13}C NMR spectrum of PPN$^+$**1c**$^-$ in THF at −80 through +50 °C showed three resonances which at 23 °C are positioned at 218.1, 203.9, and 203.0 ppm, of approximate intensities 4:1:4. These are assigned to $Fe(CO)_4$, $W(CO)_{trans}$, and $W(CO)_{cis}$, respectively.[9] The hydride chemical shifts for **1a**$^-$, **1b**$^-$, and **1c**$^-$ are (at −14.6, −11.5, and −11.8 ppm, respectively) upfield of both $HM(CO)_5^-$ and $HFe(CO)_4^-$. The observed J_{WH} of 15.0 Hz is much smaller than that for $HW(CO)_5^-$ (52.5 Hz),[6] $(\mu\text{-H})W_2(CO)_{10}^-$ (42.0 Hz), $(\mu\text{-H})WCr(CO)_5^-$ (38.4 Hz),[10] $Ph_3PAuHW(CO)_5$ (37 Hz),[5] or $(\mu\text{-H})_2W_2(CO)_8^{2-}$ (30 Hz).[11]

The X-ray crystal structure[12] of PPN$^+$**1c**$^-$ showed no bridging CO's, a structural feature similar to the parent $(\mu\text{-H})W_2(CO)_{10}^-$.

---

(1) a) Kaesz, H. D.; Saillant, R. B. *Chem. Rev.* **1972**, *72*, 231. (b) Bau, R. Ed. *ACS Symp. Ser.* **1978**, *No. 73*, 167.

(2) Bau, R.; Teller, R. G.; Kirtley, S. W.; Koetzle, T. F. *Acc. Chem. Res.* **1979**, *12*, 176.

(3) Collman, J. P.; Finke, R. G.; Matlock, P. L.; Wahren, R.; Komoto, R. G. *J. Am. Chem. Soc.* **1978**, *100*, 1119.

(4) (a) Wong, K. S.; Scheidt, W. R.; Labinger, J. A. *Inorg. Chem.* **1979**, *18*, 136. (b) Leblanc, J. C.; Reynoud, J. F.; Moise, C. *J. Organomet. Chem.* **1983**, *244*, C24.

(5) Green, M.; Orpen, A. G.; Salter, I. D.; Stone, F. G. A. *J. Chem. Soc., Chem. Commun.* **1982**, 813.

(6) Darensbourg, M. Y.; Slater, S. G. *J. Am. Chem. Soc.* **1981**, *103*, 5914.

(7) PPN$^+$ = bis(triphenylphosphine)iminium, $Ph_3P{=}N{=}PPh_3^+$.

(8) Elemental anal. (Mic Anal Organic Microanalysis, Tucson, AZ). Calcd for $Ph_3PNPPh_3^+HFeW(CO)_9^-$ (Found): C, 52.40 (52.26); H, 3.03 (3.06); N, 1.36 (1.44). ν(CO) IR (THF solution) (PPN$^+$**1a**$^-$) 2057 vw, 2012 w, 2000 m, sh, 1942 s, 1911 m, sh, 1880 m, br cm^{-1}, (PPN$^+$**1b**$^-$) 2062 vw, 2005 m, sh, 1950 s, 1922, m, 1885 m, br cm^{-1}, (PPN$^+$**1c**$^-$) 2063 vw, 2009 m, sh, 1940 s, 1911 m, sh, 1870 m, br cm^{-1}.

(9) The CO sites on Fe are presumed to be rapidly interconverting.

(10) Hayter, R. G. *J. Am. Chem. Soc.* **1966**, *88*, 4376.

(11) Lin, J. T.; Hagen, G. P.; Ellis, J. E. *J. Am. Chem. Soc.* **1983**, *105*, 2296.

(12) Data were collected on an Enraf-Nonius CAD-4 computer automated diffractometer at −103 °C using Mo Kα radiation. Space group is $P\bar{1}$ (Z = 2) with a = 14.099 (5) Å, b = 11.601 (5) Å, c = 14.148 (5) Å, α = 95.53 (3)° β = 118.23 (3)°, γ = 92.39 (3)°. Intensity data were collected for 5671 reflections, of which 3635 were unique and measured $>3\sigma(I)$ and were used for structure refinement. With a unit weighting scheme, R = 0.059.

0002-7863/84/1506-0456$01.50/0